

# Helium recombination spectra as temperature diagnostics for planetary nebulae

Y. Zhang <sup>1</sup>

*Department of Astronomy, Peking University, Beijing 100871, P. R. China*

zhangy@bac.pku.edu.cn

X.-W. Liu

*Department of Astronomy, Peking University, Beijing 100871, P. R. China*

Y. Liu

*Department of Physics, Guangzhou University, Guangzhou 510405, P. R. China*

R. H. Rubin <sup>2</sup>

*NASA Ames Research Center, Moffett Field, CA 94035-1000, USA*

## ABSTRACT

Electron temperatures derived from the He I recombination line ratios, designated  $T_e(\text{He I})$ , are presented for 48 planetary nebulae (PNe). We study the effect that temperature fluctuations inside nebulae have on the  $T_e(\text{He I})$  value. We show that a comparison between  $T_e(\text{He I})$  and the electron temperature derived from the Balmer jump of the H I recombination spectrum, designated  $T_e(\text{H I})$ , provides an opportunity to discriminate between the paradigms of a chemically homogeneous plasma with temperature and density variations, and a two-abundance nebular model with hydrogen-deficient material embedded in diffuse gas of a “normal” chemical composition (i.e.  $\sim$  solar), as the possible causes of the dichotomy between the abundances that are deduced from collisionally excited lines to those deduced from recombination lines. We find that  $T_e(\text{He I})$  values are significantly lower than  $T_e(\text{H I})$  values, with an average difference of  $\langle T_e(\text{H I}) - T_e(\text{He I}) \rangle = 4000$  K. The result is consistent with the expectation of the two-abundance nebular model but is opposite to the prediction of the scenarios

---

<sup>1</sup>Present address: Space Telescope Science Institute, 3700 San Martin Drive, Baltimore, MD 21218

<sup>2</sup>Orion Enterprises, M.S. 245-6, Moffett Field, CA 94035-1000, USA

of temperature fluctuations and/or density inhomogeneities. From the observed difference between  $T_e(\text{He I})$  and  $T_e(\text{H I})$ , we estimate that the filling factor of hydrogen-deficient components has a typical value of  $10^{-4}$ . In spite of its small mass, the existence of hydrogen-deficient inclusions may potentially have a profound effect in enhancing the intensities of He I recombination lines and thereby lead to apparently overestimated helium abundances for PNe.

*Subject headings:* ISM: general — planetary nebulae

## 1. Introduction

Two long-standing problems in nebular astrophysics are a) heavy element abundances relative to hydrogen obtained from collisionally excited lines (CELs) are generally lower than those determined from optical recombination lines (ORLs); and b) electron temperatures deduced from the collisionally excited [O III] nebular-to-auroral forbidden line ratio – hereafter  $T_e([\text{O III}])$  – are systematically higher than those determined from the Balmer jump (BJ) of H I recombination spectrum – hereafter  $T_e(\text{H I})$  – (see Liu 2003 for a recent review).

Several solutions have been proposed for the discrepancies. Peimbert (1967) showed that temperature fluctuations within nebulae can lead to a  $T_e([\text{O III}])$  which overestimates the average emission temperature of the H I recombination spectrum and the [O III] nebular lines. As a consequence, the  $\text{O}^{2+}/\text{H}^+$  ionic abundance ratio derived from the intensity ratio of the [O III] nebular lines to  $\text{H}\beta$ , assuming  $T_e([\text{O III}])$  as the electron temperature, may be grossly underestimated. The presence of temperature fluctuations will also lead to a  $T_e([\text{O III}])$  that is systematically higher than  $T_e(\text{H I})$ , the temperature derived from the H I recombination spectrum. Evidence in favor of this was first presented by Peimbert (1971) who measured values of  $T_e(\text{H I})$  in several H II regions and planetary nebulae (PNe) from the observed magnitude of the H I Balmer jump and found that they are systematically lower than the corresponding values of  $T_e([\text{O III}])$  of the same nebulae. A parameter  $t^2$  was introduced by Peimbert (1967) to characterize the magnitude of temperature fluctuations in a given nebula. The scenario has however been found to be unable to account for the low abundances derived from temperature-insensitive IR CELs. High quality measurements of IR fine-structure lines with the *Infrared Space Observatory (ISO)* for a number of PNe have shown that these lines of very low excitation energies generally yield abundances similar to the values inferred from optical/UV CELs. Again they are lower with respect to ORL abundances (e.g. Liu et al. 2000, 2004b; Tsamis et al. 2004). Moreover, recent observational studies of several samples of PNe show that typical values of  $t^2$  derived by comparing  $T_e([\text{O III}])$  and  $T_e(\text{H I})$  are so large that they are well beyond the predictions of any photoionization models (Liu & Danziger

1993; Zhang et al. 2004) unless extra energy input (such as from magnetic reconnection or from shocks) is considered.

A more plausible solution for the discrepancies of temperature and abundance determinations using CELs and ORLs is the two-component nebular model with hydrogen-deficient inclusions embedded in the diffuse nebula first proposed by Liu et al. (2000). Unlike the purely phenomenological temperature fluctuations scenario, the two-component nebular model provides a physical explanation for the temperature and abundance determination discrepancies. The model assumes that there is a small amount of H-deficient material embedded in the diffuse nebula of “normal” composition. Due to the much enhanced cooling rates by IR fine-structure lines of heavy element ions as a result of the high metallicity, hydrogen-deficient inclusions have so low an electron temperature that they emit copiously in ORLs but essentially not at all in CELs. In this scenario, the high heavy elemental abundances yielded by ORLs simply reflect the enhanced metallicity in those H-deficient inclusions, rather than representing the overall chemical composition of the whole nebula. Detailed two-abundance photoionization models incorporating H-deficient inclusions have been constructed by Péquignot et al. (2003). The models provide a satisfying explanation for the apparent large discrepancies between the results of temperature and abundance determinations using CELs and ORLs, for the PNe NGC 6153, M 1-42 and M 2-36. Contrary to the temperature fluctuations scenario, the two-component nebular model does not need any extra energy input to reproduce the large temperature inhomogeneities within PNe. On the other hand, the presence of such H-deficient inclusions is not predicted by any of the current theories of the nucleosynthesis and evolution of low- and intermediate-mass stars and their nature and origin remain unclear. One possibility is that they are evaporating icy planetesimals (Liu 2003).

More plasma diagnostic methods are helpful to probe nebular physical structure and to advance our understanding of the aforementioned fundamental problems. Earlier studies (e.g. Peimbert et al. 2000, 2002) show that temperature fluctuations can affect the intensities of He I lines. Peimbert et al. (1995) presented a method to determine the average emission temperature of He I lines, – hereafter  $T_e(\text{He I})$  – by adjusting the optical depth, the  $t^2$  parameter and electron temperature to reconcile the  $\text{He}^+/\text{H}^+$  ratios yielded by individual He I lines. The method however requires accurate atomic data in addition to high quality line intensity measurements.

Increasingly reliable atomic data are becoming available. A calculation for the effective recombination coefficients of a selection of He I lines was given by Smits (1996). Sawey & Berrington (1993) studied the contributions of collisional excitation from the  $\text{He}^0 2s^3\text{S}$  and  $2s^1\text{S}$  meta-stable levels by electron impacts to the observed fluxes of He I lines. Combining

the recombination data of Smits (1996) and the collision strengths of Sawey & Berrington (1993), Benjamin et al. (1999) presented improved He I line emission coefficients and fit the results with analytical formulae. More recently, Benjamin et al. (2002) studied the effects of the optical depth of the  $2s^3S$  meta-stable level on He I line intensities. The availability of these improved atomic data has made it possible to obtain secure measurements of  $T_e(\text{He I})$ , given high quality spectroscopic data.

The main goal of the current paper is to demonstrate that He I emission lines provide a valuable probe of nebular thermal structure and a method to discriminate different scenarios proposed as the causes of the CEL versus ORL temperature and abundance determination discrepancies. In Section 2, we present electron temperatures derived from He I lines and confront the results with the predictions of the scenarios of temperature fluctuations, density inhomogeneities and of the two-abundance nebular model in Section 3. We summarize our results in Section 4.

## 2. Electron temperatures from He I lines

### 2.1. Method and atomic data

Benjamin et al. (1999) provide analytic formulae for the emissivities of He I lines as a function of electron temperature for  $N_e = 10^2, 10^4$  and  $10^6 \text{ cm}^{-3}$ , including contributions from recombinations of  $\text{He}^+$  with electrons (Smits 1996) and from the effects of collisional excitation from the  $2s^3S$  and  $2s^1S$  meta-stable levels (Sawey & Berrington 1993). Using their formulae, the intensity ratio of two He I lines is given by

$$\frac{I_1}{I_2} = \frac{a_1}{a_2} T_{e4}^{b_1 - b_2} \exp\left(\frac{c_1 - c_2}{T_{e4}}\right), \quad (1)$$

where  $T_{e4} = T_e/10^4 \text{ K}$ . Values of the fitting parameters  $a_i$ ,  $b_i$  and  $c_i$  are given by Benjamin et al. (1999) for the temperature range 5 000–20 000 K, within which the emissivity fits have a maximum error of less than 5%. For lower temperatures, we have obtained similar fits using the numerical values given by Smits (1996) and Sawey & Berrington (1993) and present the results in Appendix A. For singlet lines, Case B recombination was assumed.

By measuring the intensity ratio of two He I recombination lines, one can in principle determine the electron temperature from Eq. (1). This is however not an easy task given the relatively weak dependence of the line ratio on temperature. Apart from recombination and collision excitation, other minor effects that can potentially affect the observed line intensities may also need to be considered, such as self-absorption from the meta-stable  $2s^3S$  level which can be significantly populated under typical nebular conditions. In order to

achieve the best measurements of the average He I line emission temperature, one needs to take into account a variety of considerations, including the strengths and ability to measure the lines involved in the ratio, the accuracy and reliability of the atomic data for the lines, the sensitivity of the ratio to  $T_e$ , and the magnitudes of contaminations by other unwanted side effects such as collisional excitation and self-absorption. After a thorough investigation, we decided that the best line ratio suitable for temperature determinations is probably the  $\lambda 7281/\lambda 6678$ , for the following reasons: 1) The  $\lambda\lambda 7281, 6678$  lines are amongst the strongest He I lines observable in the optical, after the  $\lambda 5876$  and  $\lambda 4471$  lines, and both lines fall in a spectral region clear of serious telluric absorption/emission and blending by any other known strong spectral features (see Fig. 1 for a typical nebular spectrum showing the relevant spectral region); 2) The atomic data associated with the  $\lambda\lambda 7281, 6678$  lines are amongst the best determined; 3) The He I  $\lambda 7281/\lambda 6678$  ratio is more sensitive to temperature but less sensitive to density compared to other ratios of strong He I lines; 4) Both the  $\lambda 6678$  and  $\lambda 7281$  lines are from singlet states and thus are essentially unaffected by the optical depth effects of the  $2s^3S$  level; 5) Given the small wavelength span between the  $\lambda\lambda 7281, 6678$  lines, measurements of their intensity ratio are less sensitive to any uncertainties in reddening corrections and flux calibration (c.f. also Liu et al. 2004b).

## 2.2. Results

In this work, a total of 48 PNe are analyzed. Amongst them, 23 were observed with the 4.2 m William Herschel Telescope at La Palma and the ESO 1.52 m telescope, as described in Zhang et al. (2004). For the remaining sources, spectral data are from Liu et al. (2004a), Tsamis et al. (2003a), Wesson et al. (2004), Ruiz et al. (2003) and Peimbert et al. (2004). The corresponding references are listed in the last column of Table 1.

In Fig. 2, we plot the He I  $\lambda 7281/\lambda 6678$  ratio versus  $T_e(\text{He I } \lambda 7281/\lambda 6678)$  for different electron densities. The observed He I  $\lambda 7281/\lambda 6678$  ratios along with measurement uncertainties are also overplotted. The electron densities of individual nebulae are taken from Zhang et al. (2004), Liu et al. (2004a), Tsamis et al. (2003a), Wesson et al. (2004), Ruiz et al. (2003) and Peimbert et al. (2004). The observed line fluxes have been corrected for dust extinction using reddening constants taken from the same references. The resultant electron temperatures derived from the  $\lambda 7281/\lambda 6678$  ratio are presented in Table 1. The associated uncertainties were estimated based on the line ratio measurement errors. Inspection of Fig. 2 shows that most PNe in our sample have  $T_e(\text{He I})$  less than 10 000 K. For this low temperature regime, the  $\lambda 7281/\lambda 6678$  ratio is quite insensitive to electron density. Thus our temperature determinations should be hardly affected by any uncertainties in density

measurements.

For comparison, we have also determined temperatures using the He I  $\lambda 7281/\lambda 5876$  ratio. For this ratio, additional uncertainties may arise due to the optical depth effects of the  $2s^3S$  level on the intensity of the  $\lambda 5876$  line. Based on the line emissivities given by Benjamin et al. (2002), we have also plotted in Fig. 3 one curve showing the variations of the  $\lambda 7281/\lambda 5876$  ratio as a function of  $T_e$  for the case of  $N_e = 10^4 \text{ cm}^{-3}$  and  $\tau_{3889} = 100$ , the optical depth at the centre of the He I  $2s^3S - 3p^3P^o$   $\lambda 3889$  line. Fig. 3 shows that uncertainties in  $\tau_{3889}$  may in principle lead to an error of approximately 1000 K in temperature determinations and that the uncertainty increases with increasing temperature. Values of  $T_e(\text{He I})$  derived from the  $\lambda 7281/\lambda 5876$  ratio are also tabulated in Table. 1. Possible errors caused by uncertainties in  $\tau_{3889}$  have not been included in the error estimates.

In Fig. 4, we compare electron temperatures derived from the  $\lambda 7281/\lambda 6678$  ratio and from the  $\lambda 7281/\lambda 5876$  ratio. Inspection of the figure shows that temperatures derived from the two ratios are generally in good agreement. There is however some evidence that the  $\lambda 7281/\lambda 5876$  ratio tends to yield lower temperatures. Two effects may be responsible for the small offsets. In our calculations, the possible effects of self-absorption on the intensity of the  $\lambda 5876$  line were not considered. If  $\tau_{3889} > 0$ , then our calculations may have systematically underestimated the  $\lambda 7281/\lambda 5876$  temperatures (c.f. Fig. 3). Alternatively, if there is some small departure from pure Case B to Case A recombination for the He I singlet lines, then our calculations may have underestimated temperatures derived from both ratios. But this effect is expected to be small for temperatures derived from the  $\lambda 7281/\lambda 6678$  ratio as both lines involved in the ratio are from singlet spectral terms, and as a result the effect may have largely canceled out. It is difficult to discriminate between these two possibilities. In any case, the relatively small offset between the two temperatures as shown in Fig. 4 suggests that both effects are not large and should not have affected our temperature determinations by a significant amount.

Table 1 also lists values of  $T_e(\text{H I})$ , the temperature derived from the ratio of the hydrogen Balmer discontinuity at  $3646 \text{ \AA}$  to H11  $\lambda 3770$ , taken from Zhang et al. (2004). A comparison between  $T_e(\text{He I})$  and  $T_e(\text{H I})$  is given in Fig. 5. It shows that, with the only exception of NGC 40,  $T_e(\text{He I})$  is lower than  $T_e(\text{H I})$ . The average difference between the two temperatures for the whole sample is  $\langle T_e(\text{H I}) - T_e(\text{He I}) \rangle = 4000 \text{ K}$ .

A measure of the electron temperature characterizing the He I zones can also be obtained by observing the He I discontinuity at  $3421 \text{ \AA}$ , produced by  $\text{He}^+$  recombinations to the He I  $2p^3P^o$  level (Liu & Danziger 1993). With  $T_e(\text{H I})$  and  $T_e(\text{He I})$  as free parameters, the H I and He I recombination continuum spectrum is calculated to fit the observed continuum spectrum of NGC 6153. The best fit yields  $T_e(\text{He I}) = 4000 \pm 1500 \text{ K}$  (Fig. 6), consistent

within the uncertainties with the value  $3350 \pm 1000$  K derived from the He I  $\lambda 7281/\lambda 6678$  line ratio. The He I  $\lambda 3421$  discontinuity is much weaker than the H I Balmer discontinuity and falls in a spectral region of even shorter wavelengths crowded by strong emission lines such as the O III Bowen fluorescence lines  $\lambda\lambda 3428, 3444$ , and is therefore much more difficult to measure. Nevertheless, high quality spectroscopic observations of this discontinuity should be invaluable.

### 3. Discussion

#### 3.1. Temperature fluctuations and density inhomogeneities

The discrepancy between electron temperatures derived from the [O III] forbidden line ratio and those deduced from the hydrogen Balmer jump was first discovered by Peimbert (1971) and was ascribed to temperature fluctuations within nebulae. For a nebula with small magnitude temperature fluctuations, for a given ionic species of number density  $N_i$ , the nebular thermal structure can be characterized by an average temperature  $T_0$  and a mean square temperature fluctuation parameter  $t^2$  defined as (Peimbert 1967),

$$T_0(N_i) = \frac{\int T_e N_e N_i dV}{\int N_e N_i dV} \quad (2)$$

and

$$t^2(N_i) = \frac{\int (T_e - T_0)^2 N_e N_i dV}{T_0^2 \int N_e N_i dV}. \quad (3)$$

For  $T_e(\text{H I})$  derived from the H I recombination spectrum Balmer discontinuity, it can be shown that (Peimbert 1967),

$$T_e(\text{H I}) = T_0(1 - 1.67t^2). \quad (4)$$

The deduction implicitly assumes that  $t^2 \ll 1$ .

Adopting the analytic expression for the fit of line emissivity as described in Section 2.1, we can write the flux of a He I recombination line as,

$$I(\text{He I}, \lambda_i) = \int N_e N(\text{He}^+) a_i T_{e4}^{b_i} \exp\left(\frac{c_i}{T_{e4}}\right) dV. \quad (5)$$

Then if  $t^2 \ll 1$ , one can rewrite the expression as a Taylor series expanded around the average temperature  $T_0$ , keeping only terms to the second order (Peimbert 1967),

$$\begin{aligned}
 I(\text{He I}, \lambda_i) &\approx a_i T_{04}^{b_i} \exp\left(\frac{c_i}{T_{04}}\right) \int N_e N(\text{He}^+) \\
 &\times \left\{ 1 + \left(b_i - \frac{c_i}{T_{04}}\right) \left(\frac{T_e - T_0}{T_0}\right) + \frac{1}{2} \left[ b_i(b_i - 1) - \frac{2c_i(b_i - 1)}{T_{04}} + \frac{c_i^2}{T_{04}^2} \right] \left(\frac{T_e - T_0}{T_0}\right)^2 \right\} dV,
 \end{aligned} \tag{6}$$

where  $T_{04} = T_0/10^4$  K. Then from Eqs. (2), (3) and (6), we have,

$$\begin{aligned}
 \frac{I(\text{He I}, \lambda_1)}{I(\text{He I}, \lambda_2)} &\equiv \frac{a_1}{a_2} T_{e4}(\text{He I}, \lambda_1/\lambda_2)^{b_1-b_2} \exp\left[\frac{c_1 - c_2}{T_{e4}(\text{He I}, \lambda_1/\lambda_2)}\right] \\
 &\approx \frac{a_1}{a_2} T_{04}^{b_1-b_2} \exp\left(\frac{c_1 - c_2}{T_{04}}\right) [1 + A(T_0)t^2],
 \end{aligned} \tag{7}$$

where

$$A(T_0) = \frac{1}{2} \left\{ b_1(b_1 - 1) - b_2(b_2 - 1) - 2[c_1(b_1 - 1) - c_2(b_2 - 1)] \frac{1}{T_{04}} + \frac{c_1^2 - c_2^2}{T_{04}^2} \right\}. \tag{8}$$

Introducing a parameter  $B$  and when  $|Bt^2| \ll 1$ , we can obtain from Eqs. (7)

$$\begin{cases} T_{e4}(\text{He I}, \lambda_1/\lambda_2)^{b_1-b_2} \exp\left[\frac{c_1-c_2}{T_{e4}(\text{He I}, \lambda_1/\lambda_2)}\right] \approx [T_{04}(1 - Bt^2)]^{b_1-b_2} \exp\left[\frac{c_1-c_2}{T_{04}(1-Bt^2)}\right] \\ B = T_{04}A(T_0)/[c_1 - c_2 - (b_1 - b_2)T_{04}]. \end{cases} \tag{9}$$

Thus if  $t^2 \ll 1$  and  $|Bt^2| \ll 1$ , we have

$$T_e(\text{He I}, \lambda_1/\lambda_2) \approx T_0 \left[ 1 - \frac{T_0 A(T_0)}{10^4(c_1 - c_2) - (b_1 - b_2)T_0} t^2 \right]. \tag{10}$$

In Eq. (10) the coefficient in front of  $t^2$  is a slowly varying function of  $T_0$ . For  $T_e(\text{He I}; \lambda_1/\lambda_2)$  derived from the  $\lambda 7281/\lambda 6678$  ratio, according to the He I line emissivity fit parameters  $b_1$ ,  $b_2$ ,  $c_1$  and  $c_2$  given by Benjamin et al. (1999) for  $T_e$  between 5000 and 20000 K and  $N_e = 10^4 \text{ cm}^{-3}$ , this coefficient varies between 0.97 and 1.25. For  $T_e < 5000$  K and  $N_e = 10^4 \text{ cm}^{-3}$ , using the fit parameters given in Appendix A (Table 2), we find that this coefficient varies between 1.03 and 1.22. Therefore, as an approximation, we adopt a value of 1.07 for this coefficient, as calculated for  $T_e = 10000$  K and  $N_e = 10^4 \text{ cm}^{-3}$ , and have

$$T_e(\text{He I}, \lambda 7281/\lambda 6678) \approx T_0(1 - 1.07t^2). \tag{11}$$

Under the scenario of small temperature fluctuations ( $t^2 \ll 1$ ), we can reasonably assume that  $T_0(\text{He I}) \approx T_0(\text{H I}) = T_0$  (c.f. Section 3.2 for further discussion on the legitimacy of this

assumption) and  $t^2(\text{He I}) \approx t^2(\text{H I}) = t^2$ . Consequently, a comparison of Eqs. (4) and (11) shows that  $T_e(\text{He I}, \lambda 7281/\lambda 6678) \gtrsim T_e(\text{H I})$ , which is exactly opposite to what is observed (c.f. Section 2.2, Table 1).

Using Eqs. (4) and (10), we plot in Fig. 5  $T_e(\text{H I})$  as a function of  $T_e(\text{He I}, \lambda 7281/\lambda 6678)$ , for the case of  $t^2 = 0.00, 0.04, 0.10$  and  $0.16$ , assuming a constant density of  $10^4 \text{ cm}^{-3}$ . Obviously, the differences between  $T_e(\text{H I})$  and  $T_e(\text{He I})$  are in the opposite direction to what is predicted by temperature fluctuations. It follows that the He I lines may arise from regions characterized by significantly lower temperature than that of the H I emission regions, i.e.,  $T_0(\text{He I}) < T_0(\text{H I})$ . This, however, will invalidate the condition  $t^2 \ll 1$ , and thus is beyond the scope of the description of the temperature fluctuations as originally envisioned by Peimbert (1967, 1971). A detailed discussion will be given below in Section 3.2.

Another theory that has been proposed to explain the ORL/CEL abundance determination and the BJ/CEL temperature determination discrepancies is density variations in a chemically homogeneous nebula (Rubin 1989; Viegas & Clegg 1994). In this scenario, because the [O III]  $\lambda 4363$  auroral line has a much higher critical density than the  $\lambda\lambda 4959, 5007$  nebular lines and is therefore less affected by collisional de-excitation in high density regions, the presence of such high density regions will lead to an overestimated  $T_e([\text{O III}])$  and consequently underestimated CEL abundances, analogous to the effects of temperature fluctuations. The presence of moderate density inhomogeneities in PNe is confirmed by recent observations (e.g. Zhang et al. 2004). However, given that H I and He I recombination lines are permitted transitions and therefore hardly affected by collisional de-excitation, such a scenario predicts  $T_e(\text{He I}) \sim T_e(\text{H I})$  (as long as He I zone  $\sim$  H I zone; see discussion below in section 3.2), also inconsistent with observations. We thus conclude that for a chemically homogeneous nebula, the possible presence of large density inhomogeneities also fails to explain the observed differences between  $T_e(\text{H I})$  and  $T_e(\text{He I})$ .

### 3.2. Two-abundance nebular models

The two-abundance nebular model proposed by Liu et al. (2000) assumes the existence of another component of H-deficient, ultra-cold ( $T_e \sim 10^3 \text{ K}$ ), ionized gas embedded in the diffuse gaseous nebula of “normal” (i.e.  $\sim$  solar) chemical composition. In this model emission from the H-deficient ultra-cold ionized regions has a larger contribution to the He I than to the H I lines, which are still dominated by emission from the normal component under a typical temperature of  $T_e \sim 10^4 \text{ K}$ . Thus, while the model predicts that  $T_e(\text{H I}) < T_e([\text{O III}])$ , it also predicts that  $T_e(\text{He I}) < T_e(\text{H I})$ , in agreement with observations (Liu 2003; Fig. 5).

Quantitatively, in a two-abundance nebula model, the intensity ratio of two He I lines can be written as,

$$\frac{I(\text{He I}, \lambda_1)}{I(\text{He I}, \lambda_2)} = \frac{[N_e N(\text{He}^+) \varepsilon_1 V]_h + [N_e N(\text{He}^+) \varepsilon_1 V]_l}{[N_e N(\text{He}^+) \varepsilon_2 V]_h + [N_e N(\text{He}^+) \varepsilon_2 V]_l}, \quad (12)$$

where  $\varepsilon_1$  and  $\varepsilon_2$  are the He I line emission coefficients,  $V$  is the volume of the emitting regions, and  $l$  and  $h$  refer to the low-metallicity regions (i.e. the diffuse nebula of “normal” composition) and the high-metallicity regions (i.e. the cold H-deficient inclusions). Then using the analytic fit to the He I line emissivity, we have,

$$\begin{aligned} \frac{I(\text{He I}, \lambda_1)}{I(\text{He I}, \lambda_2)} &\equiv \frac{a_1 T_{e4}(\text{He I}, \lambda_1/\lambda_2)^{b_1-b_2} \exp\left[\frac{c_1 - c_2}{T_{e4}(\text{He I}, \lambda_1/\lambda_2)}\right]}{a_2} \\ &= \frac{\mu_e \mu_{\text{He}} \omega \left[ a_1 T_{e4}^{b_1} \exp\left(\frac{c_1}{T_{e4}}\right) \right]_h + \left[ a_1 T_{e4}^{b_1} \exp\left(\frac{c_1}{T_{e4}}\right) \right]_l}{\mu_e \mu_{\text{He}} \omega \left[ a_2 T_{e4}^{b_2} \exp\left(\frac{c_2}{T_{e4}}\right) \right]_h + \left[ a_2 T_{e4}^{b_2} \exp\left(\frac{c_2}{T_{e4}}\right) \right]_l}, \end{aligned} \quad (13)$$

where  $\mu_e = (N_e)_h/(N_e)_l$  and  $\mu_{\text{He}} = [N(\text{He}^+)]_h/[N(\text{He}^+)]_l$  are the electron density and He<sup>+</sup> ionic density contrasts between the two nebular components, respectively, and  $\omega = V_h/V_l$  is the volume filling factor of the H-deficient component. Considering that the component of ultra-cold inclusions are hydrogen-deficient, the H I recombination line and continuum emission is characterized by the high temperature of the normal component, i.e.  $T_e(\text{H I}) \approx (T_e)_l$ .

Given  $(T_e)_h$ ,  $\mu_e$ ,  $\mu_{\text{He}}$  and  $\omega$ , one can thus obtain a relation between  $T_e(\text{H I})$  and  $T_e(\text{He I})$ . The current available observations are however not sufficient to provide full constraints of all four free parameters. Detailed photoionization models incorporating hydrogen-deficient inclusions have been constructed by Péquignot et al. (2003) to account for the multi-waveband observations of PNe NGC 6153, M 1-42 and M 2-36. If we make the simplified yet not unreasonable assumption that the postulated hydrogen-deficient inclusions in all PNe are of similar characteristics, then guided by the photoionization models of Péquignot et al. (2003), we assume that for all PNe analyzed in the current work,  $(T_e)_h = 1000$  K,  $\mu_e = 100$  and  $\mu_{\text{He}} = 25$ . Under these assumptions,  $T_e(\text{H I})$  as a function of  $T_e(\text{He I})$  is plotted in Fig. 5 for filling factors of  $\omega = 0, 10^{-5}, 10^{-4}$  and  $10^{-3}$ . Here line emissivity parameters ( $a_i, b_i, c_i$ ) for a density of  $N_e = 10^4$  and  $10^6 \text{ cm}^{-3}$  have been adopted for the “ $l$ ” and “ $h$ ” components, respectively. Adopting different densities however hardly affects our results since the emissivities of He I recombination lines are almost independent of electron density.

Fig. 5 shows that a small amount of hydrogen-deficient material with a filling factor  $\omega \sim 10^{-4}$  can account for the observed difference between  $T_e(\text{He I})$  and  $T_e(\text{H I})$  for most

of the sample PNe. Such a small amount of hydrogen-deficient material would be difficult to detect by direct imaging, especially in the strong background emission of the “normal component”. Note that in the two-abundance nebular model, heavy element ORLs arise almost entirely from the cold H-deficient inclusions, and their average emission temperature,  $T_e(\text{CNO Ne ORLs})$  should represent the true electron temperature prevailing in this H-deficient component. Thus one expects  $T_e(\text{CNO Ne ORLs}) \lesssim T_e(\text{He I})$  (Liu 2003), a prediction that has also been confirmed by the available limited measurements of  $T_e(\text{CNO Ne ORLs})$  (Liu 2003; Wesson et al. 2003; Tsamis et al. 2004; Liu et al. 2004b; Wesson et al. 2004). Further accurate measurements of  $T_e(\text{CNO Ne ORLs})$  are thus essential to better constrain the physical conditions prevailing in these regions. For this purpose, high S/N ratio, high spectral resolution (and preferably also high spatial resolution) spectroscopy on a large telescope is required.

An important consideration is whether the presence of a substantial  $\text{He}^{2+}$  zone in some PNe may contribute significantly to the observed large difference between  $T_e(\text{H I})$  and  $T_e(\text{He I})$ . Due to a higher heating rate and less efficient cooling, the electron temperature in the  $\text{He}^{2+}$  zone is generally higher than that in the  $\text{He}^+$  zone. This is indeed the case found from photoionization models for two PNe in our sample (NGC 7662 and NGC 3918) (Harrington et al. 1982; Clegg et al. 1987). It follows, then, that the average temperature of the  $\text{H}^+$  zone is higher than that of the  $\text{He}^+$  zone since the former encompasses both the  $\text{He}^+$  and  $\text{He}^{2+}$  zones. However, none of the photoionization models published so far that assume a chemically homogeneous medium predict a huge  $T_e(\text{H I}) - T_e(\text{He I})$  difference as much as 4000 K found in the current work. As an example, the classic photoionization model of NGC 7662 constructed by Harrington et al. (1982) yields only minute values of  $t^2(\text{H I})$  and  $t^2(\text{He I})$  and, as expected, in this model,  $T_0(\text{H I}) \approx T_e(\text{H I})$  and  $T_0(\text{He I}) \approx T_e(\text{He I})$ . The model yields  $T_0(\text{H I})$  of 12 590 K, in good agreement with the value  $T_e(\text{H I})$  of  $12\,200 \pm 600$  K deduced from the H I Balmer discontinuity. However, their model predicts a value of 11 620 K for  $T_0(\text{He I})$ , significantly higher than the value  $7690 \pm 1650$  K derived from the He I  $\lambda 7281/\lambda 6678$  line ratio. Finally, we note that the observed phenomenon of large difference between  $T_e(\text{H I})$  and  $T_e(\text{He I})$  persists in a number of low excitation PNe in our sample, such as H 1-35, Hu 2-1 and M 1-20 where the  $\text{He}^{2+}$  zone is essentially absent. As a consequence, we conclude that the presence of a  $\text{He}^{2+}$  zone in PNe of high excitation is unlikely to play a major role in causing the large  $T_e(\text{H I})$ ,  $T_e(\text{He I})$  discrepancy.

In Fig.7, we plot  $T_e(\text{H I})$  and  $T_e(\text{He I})$  against the excitation class, E.C., calculated following the formalism of Dopita & Meatheringham (1990) and tabulated in Table 1. Fig. 7 shows that there is a positive correlation between  $T_e(\text{H I})$  and the E.C.. Excluding two peculiar PNe, He 2-118 and M 2-24, we obtain a linear correlation coefficient of 0.66. This is consistent with the expectation that a hotter central star produces a higher heating rate

per photoionization, resulting in a higher nebular temperature. Fig.7 also shows a weaker correlation between  $T_e(\text{He I})$  and the E.C.. Again after excluding NGC 40 in addition to He 2-118 and M 2-24, the data yield a correlation coefficient of 0.41 between  $T_e(\text{He I})$  and the E.C.. Note that in the two-abundance nebular model, He I lines are strongly enhanced by emission from the H-deficient inclusions. As a consequence, the E.C. is no longer a good indicator of  $T_e(\text{He I})$ . Rather, in this scenario,  $T_e(\text{He I})$  will be mainly determined by the amount and properties of the postulated H-deficient inclusions, including their spatial distribution, density, chemical composition and filling factor.

It is interesting to note that amongst the sample PNe the only nebula that exhibits a higher value of  $T_e(\text{He I})$  compared to  $T_e(\text{H I})$ , i.e. opposite the predictions of the two-abundance model, is NGC 40 where  $T_e(\text{He I})$  is about 3500 K *higher* than  $T_e(\text{H I})$  (c.f. Fig.5). NGC 40 is ionized by a WC8 Wolf-Rayet central star (Smith 1969; Crowther et al. 1970). It is possible that in this particular object the nebular emission line spectrum is contaminated by emission from the strong stellar winds from the high-temperature H-deficient envelope of the central star, leading to apparently higher  $T_e(\text{He I})$  with respect to  $T_e(\text{H I})$  (c.f. Liu et al. 2004b). Further observations of this peculiar PN are needed to clarify the situation.

### 3.3. Helium abundance

All He I lines observable in the optical and UV are essentially entirely excited by radiative recombination. As a consequence, their intensities can be significantly enhanced by the presence of a small amount of ultra-cold, H-deficient inclusions, leading to an overestimated overall He/H abundance characteristic of the entire ionized region (Liu 2003, 2004). For a large sample of PNe, Zhang et al. (2004) showed that there is a positive correlation between He/H abundance and the difference between the temperature derived from the [O III] forbidden lines and from the hydrogen Balmer discontinuity, lending further support to this possibility. In the following, we present an analytical method to obtain a quantitative estimate of the possible enhancement of the He/H abundance due to the postulated presence of H-deficient inclusions in PNe. The assumptions about the two-abundance nebular model are the same as those described above in Section 3.2.

The intensity ratio of a He I recombination line to that of H $\beta$ ,  $I(\text{He I}, \lambda_i)/I(\text{H}\beta)$  observed from a nebula is given by

$$\begin{aligned} \frac{I(\text{He I}, \lambda_i)}{I(\text{H}\beta)} &= \frac{N(\text{He}^+, \lambda_i)(\varepsilon_i)_l 4861}{N(\text{H}^+)(\varepsilon_{\text{H}\beta})_l \lambda_i} \\ &= \frac{[N_e N(\text{He}^+) \varepsilon_i V]_h + [N_e N(\text{He}^+) \varepsilon_i V]_l}{[N_e N(\text{H}^+) \varepsilon_{\text{H}\beta} V]_h + [N_e N(\text{H}^+) \varepsilon_{\text{H}\beta} V]_l} \frac{4861}{\lambda_i}, \end{aligned} \quad (14)$$

where  $N(\text{He}^+, \lambda_i)/N(\text{H}^+)$  is the  $\text{He}^+/\text{H}^+$  ionic abundance ratio determined assuming a chemically homogeneous nebula. From the above equation we find,

$$\frac{N(\text{He}^+, \lambda_i)}{N(\text{H}^+)} \approx \left[ \omega \mu_e \mu_{\text{He}} \frac{(\varepsilon_i)_h}{(\varepsilon_i)_l} + 1 \right] \left[ \frac{N(\text{He}^+)}{N(\text{H}^+)} \right]_l. \quad (15)$$

For the small amount of H-deficient material as hypothesized in the two-abundance model, the average  $\text{He}^+/\text{H}^+$  ionic abundance ratio for the entire nebula is essentially identical to the value for the diffuse material, i.e.  $[N(\text{He}^+)/N(\text{H}^+)]_l$ . In such a case, the traditional method of abundance analysis assuming a chemically homogeneous nebula will overestimate the He/H abundance by a factor of  $[\omega \mu_e \mu_{\text{He}} (\varepsilon_i)_h / (\varepsilon_i)_l + 1]$ . For the representative values of  $\mu_e = 100$ ,  $\mu_{\text{He}} = 25$  and  $\omega = 10^{-4}$ , the  $\text{He}^+/\text{H}^+$  ionic abundance ratio will be overestimated by a factor of 1.25. For example, the empirical analysis of NGC 6153 by Liu et al. (2000) assuming a chemically homogeneous nebula yields a He/H elemental abundance ratio of 0.136, which is a factor of 1.35 higher than the average He/H abundance ratio for the entire ionized region derived from the detailed two-abundance photoionization modeling of this nebula by Péquignot et al. (2003). The much lower He/H abundance ratio obtained by two-abundance photoionization modeling is supported by observations of the collisional excitation dominated He I  $2s^3S - 2p^3P^o$   $\lambda 10830$  line (Liu 2003).

Many PNe are known to show enhancement of helium with respect to the Sun. For example, the average He/H ratio obtained by Kingsburgh & Barlow (1994) for a large sample of Galactic PNe is a factor of 1.35 solar. The enhancement is often ascribed to the second and third dredge-up processes that occur during the post-main-sequence evolution stages of the progenitor stars of PNe. However, the extremely high He abundances deduced for PNe such as He 2-111 (Kingsburgh & Barlow 1994) are difficult to explain by the current theories of nucleosynthesis and dredge-up processes. It is possible therefore that the very high He/H abundances observed in those extreme He-rich PNe are actually caused by the contribution of H-deficient inclusions embedded in the nebulae.

The CEL/ORL abundance discrepancy and the BJ/CEL temperature discrepancy which are ubiquitously observed amongst PNe are also found in H II regions (e.g. Tsamis et al. 2003b). The determination of  $T_e(\text{H I})$  for H II regions is much more difficult than for PNe due to the generally much lower surface brightness of H II regions and the strong contamination of scattered star light to the nebular spectrum in dusty H II regions. Recently, Garcia-Rojas et al. (2004) presented deep echelle spectroscopy of the Galactic H II region NGC 3576, covering the wavelength range from 3100–10400 Å. They derived  $T_e(\text{H I})$  of  $6650 \pm 750$  K and  $T_e([\text{O III}])$  of  $8500 \pm 50$  K, in agreement with the general pattern observed amongst PNe that  $T_e(\text{H I})$  is systematically lower than  $T_e([\text{O III}])$ . On the other hand, from the He I  $\lambda\lambda 6678, 7281$  line fluxes reported in their paper, we obtain  $T_e(\text{He I})$  of  $6800 \pm 600$  K, which

is consistent with  $T_e(\text{H I})$  within the errors. Note that NGC 3576 has a relatively small ORL/CEL abundance discrepancy (a factor of 1.8; Tsamis et al. 2003a; Garcia-Rojas et al. 2004). Measurements of  $T_e(\text{H I})$  and  $T_e(\text{He I})$  in more H II regions are needed, especially for those exhibiting large ORL/CEL abundance discrepancies in order to have a better picture of this problem in H II regions.

For a few metal poor extragalactic H II regions, Peimbert et al. (2002) find that the electron temperatures derived from He I recombination lines are also systematically lower than the corresponding values deduced from the [O III] forbidden line ratio. If we ascribe the discrepancy to the presence of H-deficient inclusions in these nebulae, then the effects of these inclusions on the determination of the primordial helium abundance can be estimated roughly from Eqs. (13) and (15). Using the line fluxes presented by Peimbert et al. (2002) and assuming that the H-deficient material in these metal-poor H II regions have similar composition as those postulated to exist in PN NGC 6153, we estimate that the primordial He abundance could have been overestimated by as much as 5%.

#### 4. Conclusions

In this paper, we show that He I recombination lines can be used to probe nebular thermal structures and provide vital information regarding the nature and physical causes of the long-standing ORL/CEL temperature and abundance determination discrepancies. We present electron temperatures derived from the He I  $\lambda 7281/\lambda 6678$  ratio for 48 PNe. The He I temperatures are found to be systematically lower than those deduced from the Balmer jump of the H I recombination spectrum. The result is exactly opposite to the predictions of the scenarios of temperature fluctuation and density inhomogeneities but in good agreement with the expectations of the two-abundance nebular model proposed by Liu et al. (2000). We estimate that a filling factor of the order of  $10^{-4}$  of the ultra-cold, H-deficient material is sufficient to explain the observed differences between the H I and He I temperatures. We show that the possible presence of H-deficient inclusions in PNe may indicate that current estimates of He/H abundances in PNe may have been overestimated by a factor of  $\sim 1.25$ . The possible existence of hydrogen-deficient inclusions in H II regions could also cause the primordial helium abundance determined from metal-poor H II galaxies to be overestimated. We stress the importance of high S/N ratio, high resolution spectroscopy in the tackling of these fundamental problems.

We thank the referee, Dr. V. Luridiana, for helpful suggestions and incisive comments that improved the paper significantly. YZ acknowledges the award of a Liu Yongling Scholar-

ship. Support for RHR was from the NASA Long-Term Space Astrophysics (LTSA) program.

### A. He I line emissivities ( $T_e < 5000$ K)

Combining the He I recombination model of Smits (1996) and the collisional excitation rates of Sawey & Berrington (1993), we have calculated emissivities for the He I  $\lambda\lambda 4471, 5876, 6678$  and  $7281$  lines for  $T_e < 5000$  K – the temperature range not considered by Benjamin et al. (1999). At such low temperatures, the effects of collisional excitation are however essentially negligible. We may write, following the analytic expression used by Benjamin et al. (1999),

$$\varepsilon_i = a_i T_{e4}^{b_i} \exp(c_i/T_{e4}) \text{ erg cm}^3 \text{ s}^{-1}, \quad (\text{A1})$$

where  $T_{e4} = T_e/10^4$  K, and  $a_i$ ,  $b_i$  and  $c_i$  are constants. The constants were derived using a least-squares algorithm. The results are tabulated in Table 2 for electron densities of  $N_e = 10^2, 10^4$  and  $10^6 \text{ cm}^{-3}$ . The maximum errors of the fits for the temperature range  $312.5 - 5000$  K,  $e_i$ , are also listed in the last column of the Table.

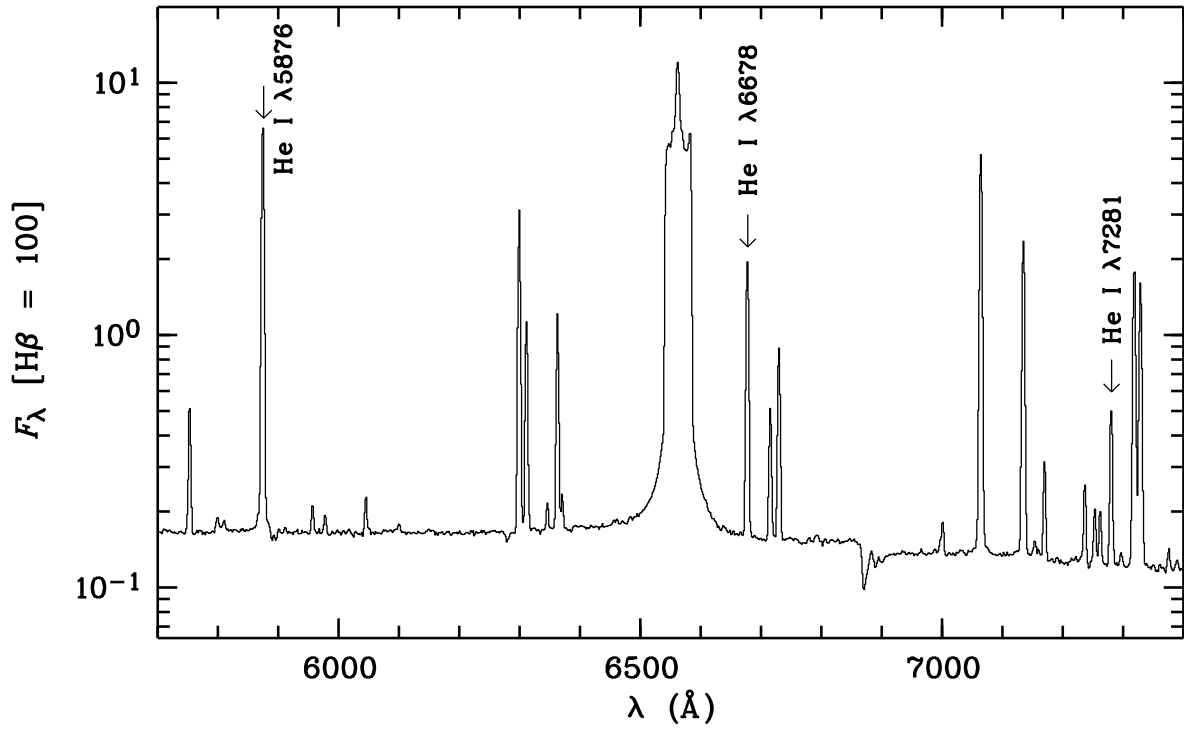


Fig. 1.— Spectrum of NGC 7009 showing the He I  $\lambda$ 5876, 6678 and 7281 lines used to determine average emission temperatures of the He I recombination spectrum. The intensity was scaled such that  $F(\text{H}\beta) = 100$ . Note that H $\alpha$  was heavily saturated in this spectrum.

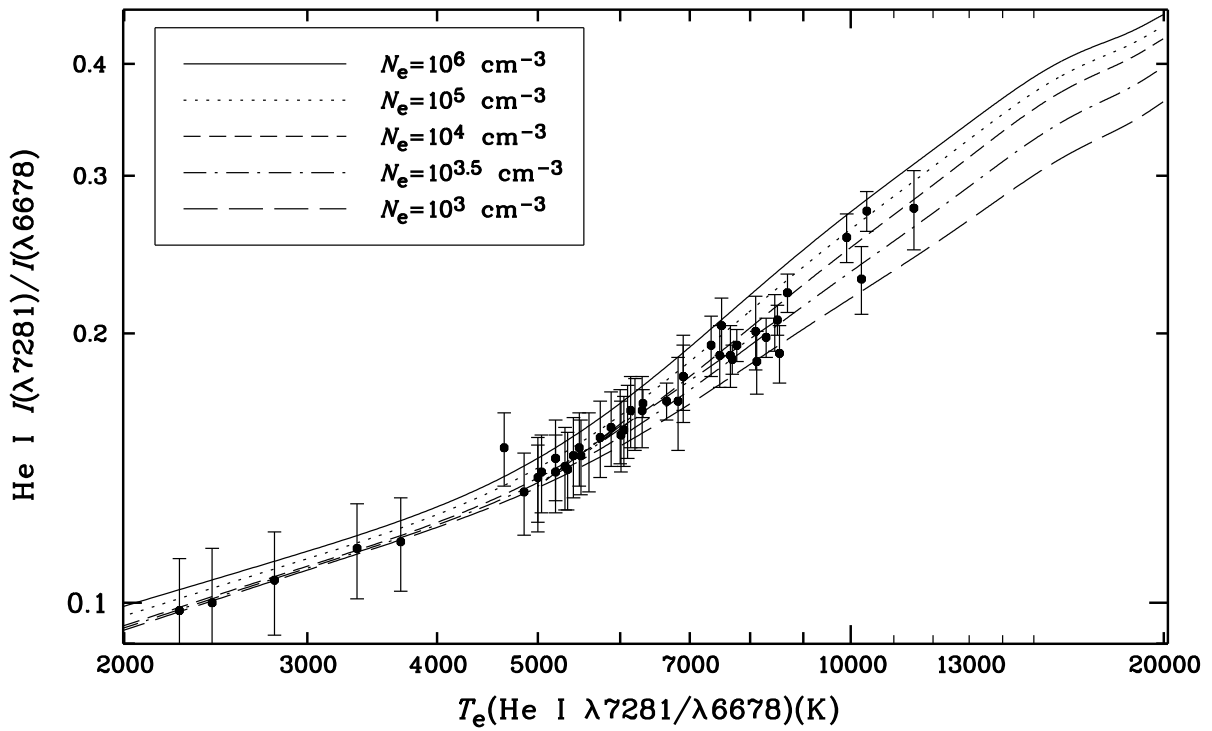


Fig. 2.— The He I  $\lambda 7281/\lambda 6678$  intensity ratio as a function of  $T_e$  for electron densities from  $N_e = 10^3$  to  $10^6 \text{ cm}^{-3}$ . The observed ratios along with their uncertainties for our sample PNe are overplotted.

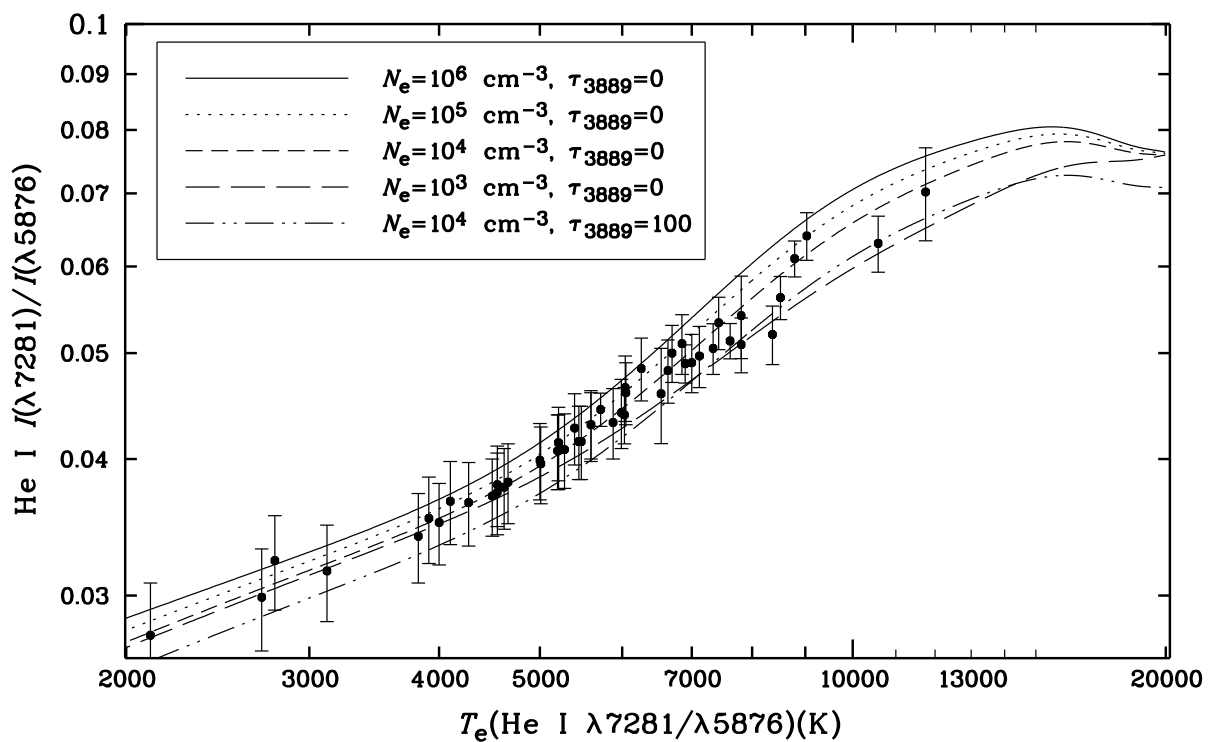


Fig. 3.— The He I  $\lambda 7281/\lambda 5876$  intensity ratio is plotted against  $T_e$  for densities from  $N_e = 10^3$  to  $10^6 \text{ cm}^{-3}$ . All curves are for zero  $\lambda 3889$  line optical depth except one for which  $\tau_{3889} = 100$  and  $N_e = 10^4 \text{ cm}^{-3}$  (see text for more details).

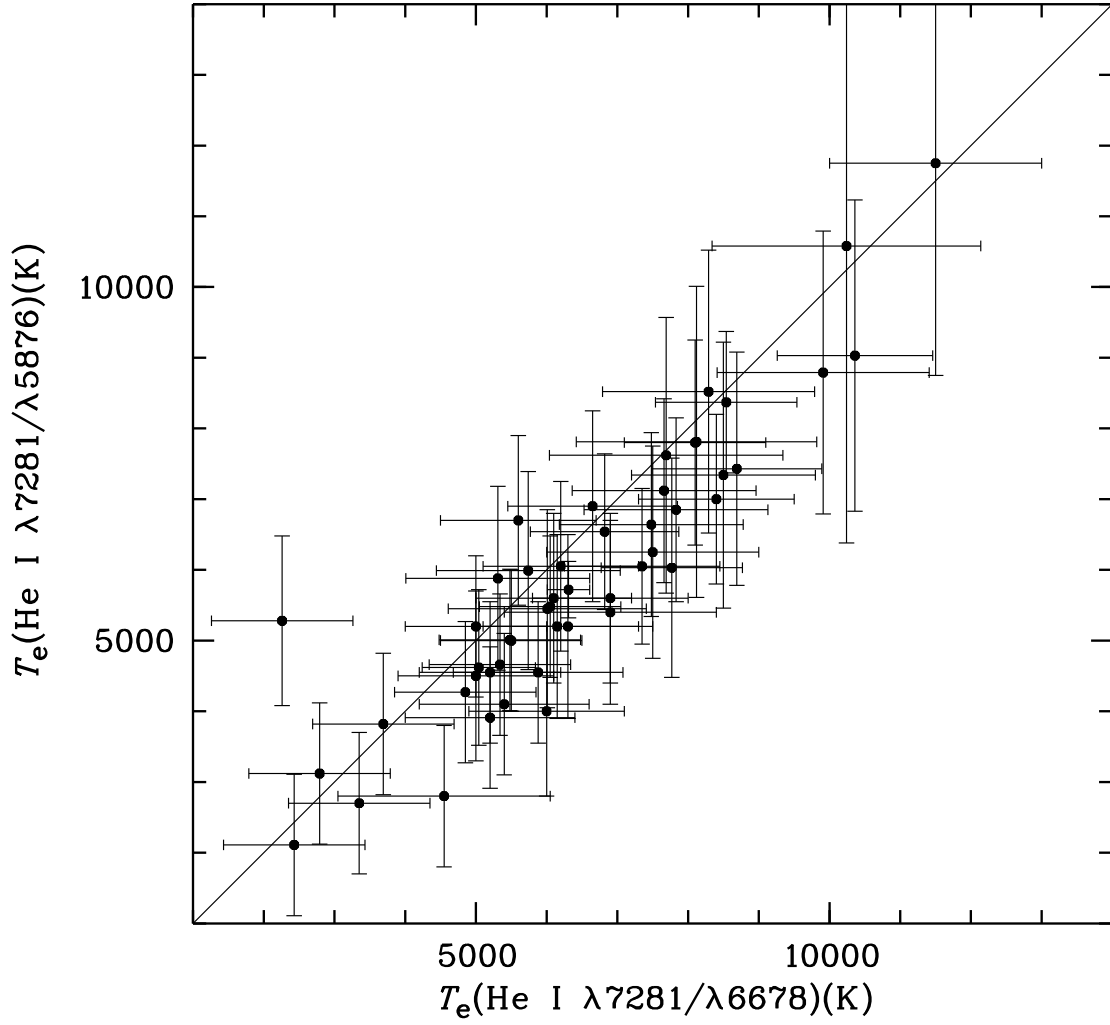


Fig. 4.— Comparison of electron temperatures derived from the He I  $\lambda 7281/\lambda 6678$  ratio with those derived from the He I  $\lambda 7281/\lambda 5876$  ratio. The diagonal line is a  $y = x$  plot.

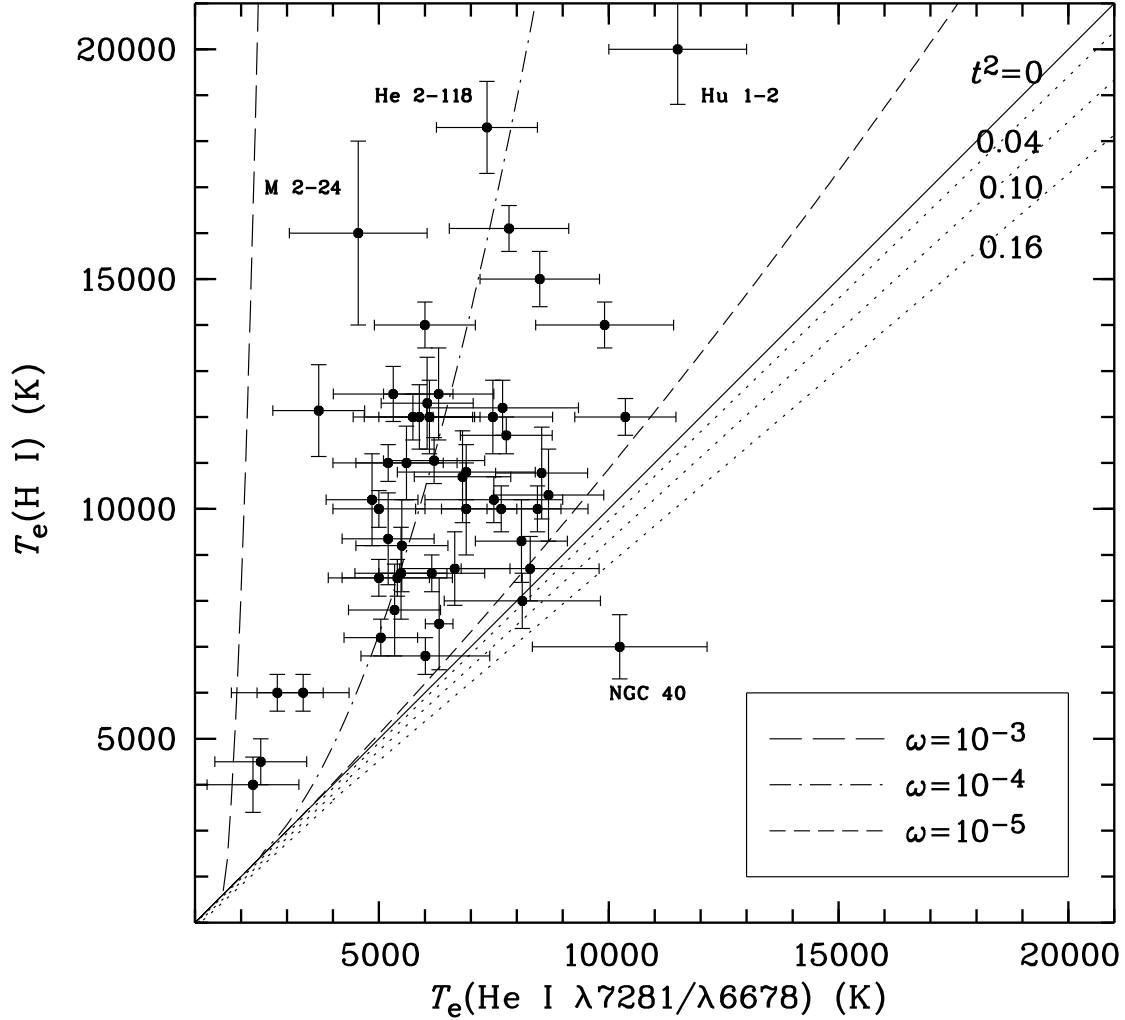


Fig. 5.—  $T_e(\text{He I})$  versus  $T_e(\text{H I})$ . The solid diagonal line is a  $y = x$  plot. The dotted lines show the variations of  $T_e(\text{H I})$  as a function of  $T_e(\text{He I})$  for mean square temperature fluctuation parameter  $t^2 = 0.04, 0.10$  and  $0.16$ , assuming a constant electron density of  $10^4 \text{ cm}^{-3}$ . The short-dashed, dot-dashed and long-dashed lines show the variations of  $T_e(\text{H I})$  as a function of  $T_e(\text{He I})$  for  $\omega = 10^{-5}, 10^{-4}$  and  $10^{-3}$ , respectively, where  $\omega$  is the volume filling factor of H-deficient inclusions.

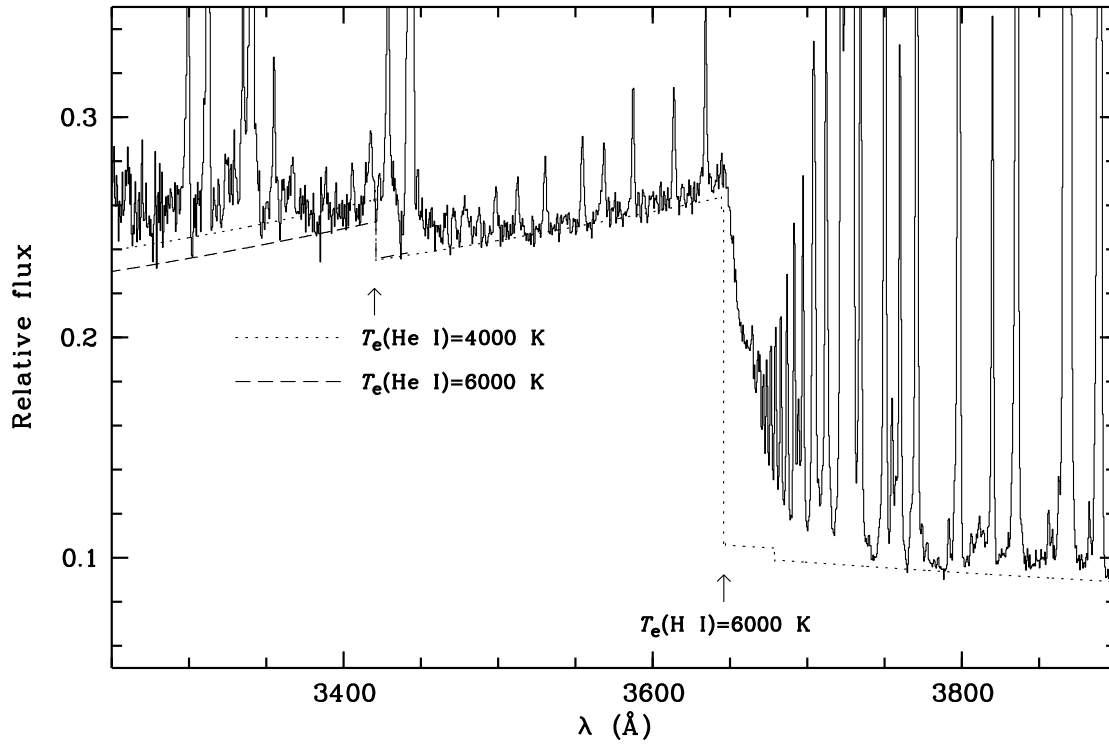


Fig. 6.— Spectrum of NGC 6153 from 3250–3900 Å, showing the He I discontinuity at 3421 Å and the H I discontinuity at 3646 Å. The dotted line is a theoretical nebular continuum spectrum calculated assuming a He I temperature of 4000 K and a H I temperature of 6000 K. For comparison, a theoretical spectrum assuming a He I temperature of 6000 K is also given (dashed line), which clearly yields a poorer fit to the observed magnitude of the He I  $\lambda$ 3421 discontinuity than the dotted line.

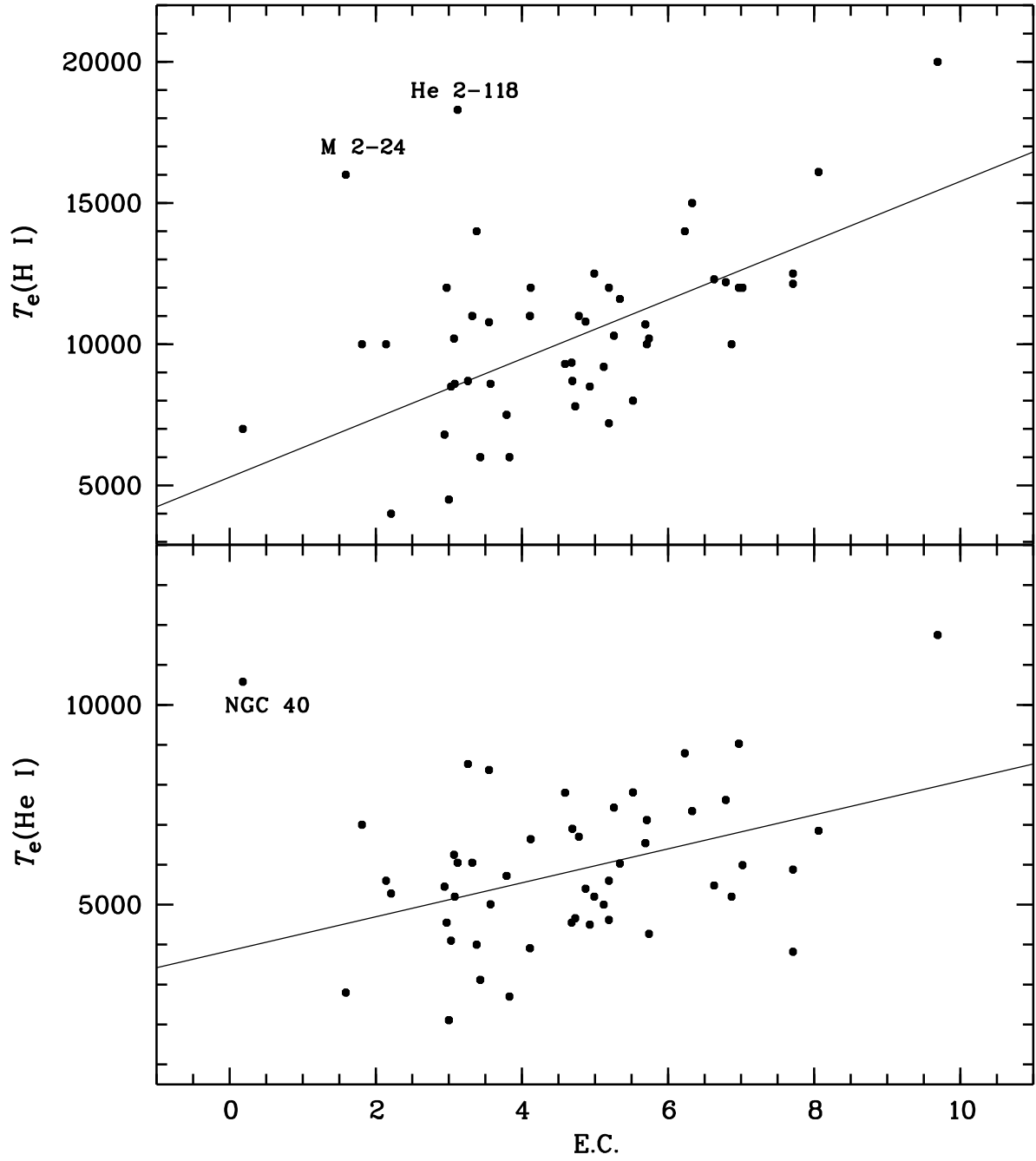


Fig. 7.— a)  $T_e(\text{H I})$  and b)  $T_e(\text{He I})$  versus Excitation Class (E.C.). The solid lines are linear least-squares fits.

Table 1. Electron temperatures derived from He I line ratios.

Source	$T_e(\text{He I } \lambda 7281/\lambda 6678)$	$T_e(\text{He I } \lambda 7281/\lambda 5876)$	$T_e(\text{H I})$	E.C.	Ref.
Cn 2-1	$6900 \pm 1500$	$5400 \pm 1300$	$10800 \pm 600$	4.87	...
H 1-35	$6900 \pm 1100$	$5600 \pm 1200$	$10000 \pm 1000$	2.14	...
H 1-50	$6300 \pm 1200$	$5200 \pm 1300$	$12500 \pm 1000$	4.99	...
He 2-118	$7350 \pm 1100$	$6050 \pm 1100$	$18300 \pm 1000$	3.12	...
Hu 1-2	$11500 \pm 1500$	$11750 \pm 3000$	$20000 \pm 1200$	9.69	L04
Hu 2-1	$8400 \pm 1100$	$7000 \pm 1200$	$10000 \pm 500$	1.81	W04
IC 1297	$5000 \pm 1000$	$5200 \pm 1000$	$10000 \pm 400$	6.87	...
IC 2003	$5600 \pm 1100$	$6700 \pm 1200$	$11000 \pm 800$	4.78	W04
IC 3568	$8100 \pm 1000$	$7800 \pm 1450$	$9300 \pm 900$	4.59	L04
IC 4191	$5500 \pm 1000$	$5000 \pm 1000$	$9200 \pm 1000$	5.12	T03
IC 4406	$5200 \pm 1000$	$4550 \pm 1000$	$9350 \pm 1000$	4.68	T03
IC 4634	$5400 \pm 1200$	$4100 \pm 1000$	$8500 \pm 400$	3.03	...
IC 4776	$6150 \pm 1150$	$5200 \pm 1300$	$8600 \pm 400$	3.08	...
IC 4997	$7500 \pm 1500$	$6250 \pm 1500$	$10200 \pm 500$	3.07	...
IC 5217	$6100 \pm 1100$	$5600 \pm 1200$	$12000 \pm 800$	5.19	W04
M 1-20	$5880 \pm 1200$	$4550 \pm 1000$	$12000 \pm 700$	2.97	...
M 1-42	$2260 \pm 1000$	$5280 \pm 1200$	$4000 \pm 600$	2.21	...
M 2-24	$4550 \pm 1500$	$2800 \pm 1000$	$16000 \pm 2000$	1.59	...
M 2-36	$2790 \pm 1000$	$3120 \pm 1000$	$6000 \pm 400$	3.43	...
M 3-21	$5200 \pm 1200$	$3910 \pm 1000$	$11000 \pm 400$	4.11	...
M 3-32	$2430 \pm 1000$	$2110 \pm 1000$	$4500 \pm 500$	3.00	...
Me 2-2	$6200 \pm 1100$	$6050 \pm 1200$	$11000 \pm 500$	3.32	W04
NGC 40	$10240 \pm 1900$	$10580 \pm 4200$	$7000 \pm 700$	0.18	L04
NGC 3132	$8540 \pm 1000$	$8370 \pm 1000$	$10780 \pm 1000$	3.55	T03
NGC 3242	$4850 \pm 1000$	$4270 \pm 1000$	$10200 \pm 1000$	5.74	T03
NGC 3918	$6050 \pm 1000$	$5480 \pm 1000$	$12300 \pm 1000$	6.63	T03
NGC 5307	$6820 \pm 1050$	$6540 \pm 1100$	$10700 \pm 1000$	5.69	R03
NGC 5315	$5480 \pm 1000$	$5010 \pm 1000$	$8600 \pm 1000$	3.57	T03
NGC 5315	$6310 \pm 300$	$5720 \pm 400$	$7500 \pm 1000$	3.79	P04
NGC 5873	$5740 \pm 1300$	$5990 \pm 1400$	$12000 \pm 500$	7.02	...
NGC 5882	$5340 \pm 1000$	$4660 \pm 1000$	$7800 \pm 1000$	4.73	T03

Table 1—Continued

Source	$T_e(\text{He I } \lambda 7281/\lambda 6678)$	$T_e(\text{He I } \lambda 7281/\lambda 5876)$	$T_e(\text{H I})$	E.C.	Ref.
NGC 6153	$3350 \pm 1000$	$2700 \pm 1000$	$6000 \pm 400$	3.83	...
NGC 6210	$6650 \pm 1200$	$6900 \pm 1350$	$8700 \pm 800$	4.69	L04
NGC 6302	$7830 \pm 1300$	$6850 \pm 1300$	$16100 \pm 500$	8.06	...
NGC 6543	$6010 \pm 1400$	$5450 \pm 1400$	$6800 \pm 400$	2.94	...
NGC 6567	$7480 \pm 1300$	$6640 \pm 1300$	$12000 \pm 800$	4.12	...
NGC 6572	$8690 \pm 1200$	$7430 \pm 1650$	$10300 \pm 1000$	5.26	L04
NGC 6620	$7660 \pm 1300$	$7120 \pm 1300$	$10000 \pm 500$	5.71	...
NGC 6720	$8120 \pm 1700$	$7810 \pm 2200$	$8000 \pm 600$	5.52	L04
NGC 6741	$8500 \pm 1300$	$7340 \pm 1880$	$15000 \pm 600$	6.33	L04
NGC 6790	$9910 \pm 1500$	$8790 \pm 2000$	$14000 \pm 500$	6.23	L04
NGC 6803	$5000 \pm 1100$	$4500 \pm 1200$	$8500 \pm 400$	4.93	W04
NGC 6833	$6000 \pm 1100$	$4000 \pm 1200$	$14000 \pm 500$	3.38	W04
NGC 6818	$3690 \pm 1000$	$3820 \pm 1000$	$12140 \pm 1000$	7.71	T03
NGC 6818	$5310 \pm 1300$	$5880 \pm 1300$	$12500 \pm 600$	7.71	...
NGC 6826	$8290 \pm 1500$	$8520 \pm 2000$	$8700 \pm 700$	3.26	L04
NGC 6884	$7770 \pm 1000$	$6030 \pm 1550$	$11600 \pm 400$	5.34	L04
NGC 7009	$5040 \pm 800$	$4620 \pm 1100$	$7200 \pm 400$	5.19	...
NGC 7027	$10360 \pm 1100$	$9030 \pm 2200$	$12000 \pm 400$	6.97	...
NGC 7662	$7690 \pm 1650$	$7620 \pm 1950$	$12200 \pm 600$	6.79	L04

References. — [L04] Liu et al. (2004a); [P04] Peimbert et al. (2004); [R03] Ruiz et al. (2003); [T03] Tsamis et al. (2003a); [W04] Wesson et al. (2004)

Table 2. Fitting parameters for He I line emissivities.

Emissivities	$a_i$	$b_i$	$c_i$	$e_i$
$N_e=10^2 \text{ cm}^{-3}$				
$j_{4471}$	$6.835 \times 10^{-26}$	-0.8224	-0.0074	1.40%
$j_{5876}$	$1.838 \times 10^{-25}$	-0.9745	-0.0086	1.11%
$j_{6678}$	$5.251 \times 10^{-26}$	-0.9819	-0.0088	1.24%
$j_{7281}$	$9.104 \times 10^{-27}$	-0.5594	0.0007	0.25%
$N_e=10^4 \text{ cm}^{-3}$				
$j_{4471}$	$6.775 \times 10^{-26}$	-0.8270	-0.0041	1.50%
$j_{5876}$	$1.824 \times 10^{-25}$	-0.9702	-0.0068	1.14%
$j_{6678}$	$5.203 \times 10^{-26}$	-0.9767	-0.0068	1.23%
$j_{7281}$	$9.463 \times 10^{-27}$	-0.5289	0.0068	1.14%
$N_e=10^6 \text{ cm}^{-3}$				
$j_{4471}$	$6.746 \times 10^{-26}$	-0.8337	0.0067	1.23%
$j_{5876}$	$1.819 \times 10^{-25}$	-0.9509	0.0035	1.37%
$j_{6678}$	$5.185 \times 10^{-26}$	-0.9581	0.0035	1.67%
$j_{7281}$	$9.663 \times 10^{-27}$	-0.5307	0.0179	2.29%

## REFERENCES

- Benjamin, R. A., Skillman, E. D., & Smits, D. P. 1999, *ApJ*, 514, 307
- Benjamin, R. A., Skillman, E. D., & Smits, D. P. 2002, *ApJ*, 569, 288
- Clegg, R. E. S., Harrington, J. P., Barlow, M. J., & Walsh, J. R. 1987, *ApJ*, 314, 551
- Crowther, P. A., De Marco, O., & Barlow, M. J. 1998, *MNRAS*, 296, 36
- Dopita, M. A., & Meatheringham, S. J. 1990, *ApJ*, 357, 140
- Garcia-Rojas, J., Esteban, C., Peimbert, M., Rodríguez, M., Ruiz, M. T., & Peimbert, A. 2004, *ApJ*, 153, 501
- Harrington, J. P., Seaton, M. J., Adams, S., & Lutz, J. H. 1982, *MNRAS*, 199, 517
- Kingsburgh, R. L., & Barlow, M. J. 1994, *MNRAS*, 271, 257
- Liu, X.-W. 2003, in *IAU Symp. 209, Planetary Nebulae*, eds. S. Kwok, M. Dopita, R. Sutherland (San Francisco: ASP), p.339
- Liu, X.-W. 2004, in *Planetary Nebulae beyond the Milky Way*, eds. J. Walsh, L. Stanghellini and N. Douglas (ESO, Garching bei München), in press
- Liu, X.-W., & Danziger, I. J. 1993, *MNRAS*, 263, 256
- Liu, X.-W., Luo, S.-G., Barlow, M. J., Danziger, I. J., & Storey P. J. 2001, *MNRAS*, 327, 141
- Liu, X.-W., Storey, P. J., Barlow, M. J., Danziger, I. J., Cohen, M., & Bryce, M. 2000, *MNRAS*, 312, 585
- Liu, Y., Liu, X.-W., Luo, S.-G. & Barlow, M. J. 2004a, *MNRAS*, 353, 1231
- Liu, Y., Liu, X.-W., Barlow, M. J., & Luo, S.-G. 2004b, *MNRAS*, 353, 1251
- Peimbert, A., Peimbert, M., & Luridiana, V. 2002, *ApJ*, 565, 668
- Peimbert, M. 1967, *ApJ*, 150, 825
- Peimbert, M. 1971, *Bol. Obs. Tonantzintla Tacubaya*, 6, 29
- Peimbert, M., Luridiana, V., & Torres-Peimbert, S. 1995, *RevMaxAA*, 31, 147
- Peimbert, M., Peimbert, A., & Ruiz, M. T. 2000, *ApJ*, 541, 688

- Peimbert, M., Peimbert, A., Ruiz, M. T., & Esteban, C. 2004, *ApJ*, 150, 431
- Péquignot, D., Liu, X.-W., Barlow, M. J., Storey, P. J., & Morisset, C. 2003, in *IAU Symp. 209, Planetary Nebulae*, eds. S. Kwok, M. Dopita, R. Sutherland (San Francisco: ASP), p.347
- Rubin, R. H. 1989, *ApJS*, 69, 897
- Ruiz, M. T., Peimbert, A., Peimbert, M., & Esteban, C. 2003, *MNRAS*, 340, 362
- Sawey, P. M. J., & Berrington, K. A. 1993, *At. Data Nucl. Data Tables*, 55, 81
- Smith, L. F., & Aller, L. H. 1969, *ApJ*, 157, 1245
- Smits, D. P. 1996, *MNRAS*, 278, 683
- Tsamis, Y. G., Barlow, M. J., Liu, X.-W., Danziger, I. J., & Storey, P. 2003a, *MNRAS*, 345, 186
- Tsamis, Y. G., Barlow, M. J., Liu, X.-W., Danziger, I. J., & Storey, P. 2003b, *MNRAS*, 338, 678
- Tsamis, Y. G., Barlow, M. J., Liu, X.-W., Storey, P. & Danziger, I. J. 2004, *MNRAS*, 353, 953
- Viegas, S. M., & Clegg, E. S. 1994, *MNRAS*, 271, 993
- Wesson, R., Liu, X.-W., & Barlow, M. J. 2003, *MNRAS*, 340, 253
- Wesson, R., Liu, X.-W., & Barlow, M. J. 2004, *MNRAS*, submitted
- Zhang, Y., Liu, X.-W., Wesson, R., et al. 2004, *MNRAS*, 351, 935